JTTEE5 19:1074–1080
DOI: 10.1007/s11666-010-9505-0
1059-9630/$19.00 © ASM International

Oxidation Behavior of ZrO_2 Reinforced $MoSi_2$ Composite Coatings Fabricated by Vacuum Plasma Spraying Technology

Xiaoai Fei, Yaran Niu, Heng Ji, Liping Huang, and Xuebin Zheng

(Submitted December 24, 2009; in revised form March 9, 2010)

In this work, $MoSi_2$, $MoSi_2$-20 vol.% ZrO_2, $MoSi_2$-40 vol.% ZrO_2 (denoted, respectively, as MZ0, MZ2, and MZ4) coatings were fabricated by vacuum plasma spraying technology. The oxidation behavior of the coatings was examined at 500, 1200, and 1500 °C, respectively. Some basic properties of the coatings, including microhardness, porosity, and surface roughness were characterized. The tests at 500 °C showed that the pest oxidation phenomenon of $MoSi_2$ coatings was restrained by the addition of ZrO_2. The MZ2 coating exhibited excellent oxidation-resistant behavior both at 1200 and 1500 °C. However, the MZ4 coating presented the impaired oxidation-resistant behavior at 1500 °C, though the comparable oxidation property at 1200 °C was still obtained.

Keywords microstructure, $MoSi_2$, oxidation resistance, vacuum plasma spraying, ZrO_2

1. Introduction

Intermetallics like silicides have been extensively evaluated for high-temperature structural applications and considerable attention has been directed toward refractory metal silicides (Ref 1). Molybdenum disilicide ($MoSi_2$) is a leading candidate for high-temperature application due to its good oxidation resistance at elevated temperature, relatively low density and coefficient of thermal expansion, high-thermal conductivity and thermodynamic compatibility with a wide variety of potential ceramic reinforcements (Ref 2). The excellent oxidation resistance of $MoSi_2$ comes from the formation of a continuous SiO_2 film on its surface, which protects the materials from further oxidation (Ref 3).

Many studies have revealed that $MoSi_2$ could be used as protective coating material on various substrates and many methods have been applied to fabricate $MoSi_2$ coatings. Several surface treatment processes, such as chemical vapor deposition, pack siliconizing, and vacuum sintering, have been applied to deposit $MoSi_2$ onto Mo substrate for protecting the substrate from oxidation at high temperature (Ref 4).

Xiaoai Fei, Yaran Niu, Heng Ji, Liping Huang, and **Xuebin Zheng**, Key Laboratory of Inorganic Coating Materials, Chinese Academy of Sciences, Shanghai 200050, China and Shanghai Institute of Ceramics, Chinese Academy of Sciences, Shanghai 200050, China. Contact e-mails: xbzheng@mail.sic.ac.cn and xiaoaif@yahoo.cn.

Unfortunately, there are some disadvantages of monolithic $MoSi_2$ coatings, such as pest oxidation under low temperature (around 500 °C). Catastrophic nature of the pest oxidation was proposed to occur through transport of oxygen into the interior of $MoSi_2$ along preexisting cracks, grain boundaries, and/or pores, which was accomplished with volume expansion of about 250% (Ref 5). Another problem is the high porosity (Ref 6). Several methods have been developed to solve the drawbacks of $MoSi_2$ coatings, among which the fabrication of composite coatings is potentially useful (Ref 7).

ZrO_2 is a very attractive alternative reinforcing species for $MoSi_2$. The addition of ZrO_2 into $MoSi_2$ may block the path of oxygen diffusion, therefore restrain the pest oxidation (Ref 8). Besides, the addition of appropriate amount of ZrO_2 progressively refined the grain size of $MoSi_2$ by retarding its grain growth during the crystallization, which improved the density of $MoSi_2$ (Ref 9). Furthermore, the thermal expansion coefficient of ZrO_2 (9.6×10^{-6} K^{-1}) is close to that of $MoSi_2$ (7.8×10^{-6} K^{-1}), suggesting thermocompatibility of the two materials, consequently, ZrO_2 has been used to reinforce bulk $MoSi_2$ (Ref 10).

In this work, $MoSi_2$-ZrO_2 composite coatings as well as monolithic $MoSi_2$ coatings were fabricated by vacuum plasma spraying (VPS) technology. The microstructures of the coatings were characterized by scanning electron microscopy (SEM) and X-ray diffraction (XRD). Microhardness, porosity, and surface roughness of the coatings were evaluated. The oxidation behavior of the coatings was checked at 500, 1200, and 1500 °C, respectively.

2. Experimental Procedure

2.1 Materials and Preparation

Commercial $MoSi_2$ (Zhengzhou Chida Tungsten & Molybdenum Products Co., Ltd., Zhengzhou, China) and

ZrO_2 (with 7-8 wt% Y_2O_3) (Anyan Tianchuang Hot Spray Products Co., Ltd., Anyan, China) powders were chosen in the size range of 10-60 μm. $MoSi_2$ powders with 20 and 40 vol.% ZrO_2 were, respectively, mechanically mixed in a ball mill machine for 12 h, then dried at 110 °C for 2 h.

The deposition of coatings was carried out with a VPS equipment (F4-VB, Sulzer Metco AG, Wohlen, Switzerland). The optimized parameters are summarized in Table 1. Free-standing coatings of thickness about 0.5-1.0 mm were fabricated for the following examinations.

2.2 Composition and Microstructure Characterization

The crystalline phases of the starting powders and as-received coatings were analyzed by XRD (RAX-10, Rigaku, Japan) operating with Cu Kα ($\lambda = 1.5406$ nm) radiation. The surface and cross section morphologies of the as-sprayed and heat-treated coatings were investigated by field emission scanning electron microscopy (FESEM, JSM-6700F, JEOL, Tokyo, Japan). The chemical composition of coatings was identified by energy dispersive spectrometer (EDS, PN-5502, INCA ENERGY, Oxford, UK).

The microhardness measurements were conducted on the cross section of the as-sprayed coatings using a microhardness instrument (HX-100, Shanghai Second Optical Instrument Factory, Shanghai, China) under loading weight 4.9 N and duration time 15 s. The value obtained represented an average of 20 point measurements. The porosity of the coatings was measured by an image analysis system on the polished cross sections using a software (IMAGE, National Institute of Health, Bethesda, USA). Three duplicate measurements were carried out for each sample. Surface roughness was measured by HOMMEL WERKE (T8000, Wave, Villingen-Schwenningen, Germany). Twenty measurements were carried out for each sample.

2.3 Oxidation Behavior Characterization

The free-standing coatings were, respectively, tested at 500, 1200, and 1500 °C to investigate their oxidation behavior. For the oxidation tests at 500 and 1200 °C, the specimens were placed in an alumina crucible in a tube type furnace, the samples were put inside or taken out of the furnace directly to air within several seconds. For the oxidation tests at 1500 °C, the specimens were placed in an alumina crucible in a box-type furnace, the samples were furnace-heated and cooled by 5 K/min.

Table 1 Vacuum plasma spray parameters of $MoSi_2$-ZrO_2 coatings

Parameters	Values
Power, kW	35
Gas Ar, slpm	42
Gas H_2, slpm	10
Spraying distance, mm	300
Carrier gas Ar, slpm	4
Pressure, mbar	100

3. Results and Discussion

3.1 Microstructure Characterization of the As-Sprayed Coatings

The XRD patterns of the starting powders and as-sprayed coatings are shown in Fig. 1. Tetragonal $MoSi_2$ could be found in all of the three kinds of powders. At the same time, additional tetragonal and cubic ZrO_2 phases were detected in the MZ2 and MZ4 powders (Fig. 1a). The XRD patterns of the MZ0, MZ2, and MZ4 coatings show that tetragonal $MoSi_2$ has been converted to hexagonal $MoSi_2$ after the spraying process. Further, a small amount of Mo_5Si_3 was detected in all of the three kinds of coatings. It was thought that due to the ultrahigh temperature of plasma plume and high-cooling rate of the molten particles during the spraying process, the high-temperature hexagonal $MoSi_2$ was kept as the main phase in the coatings.

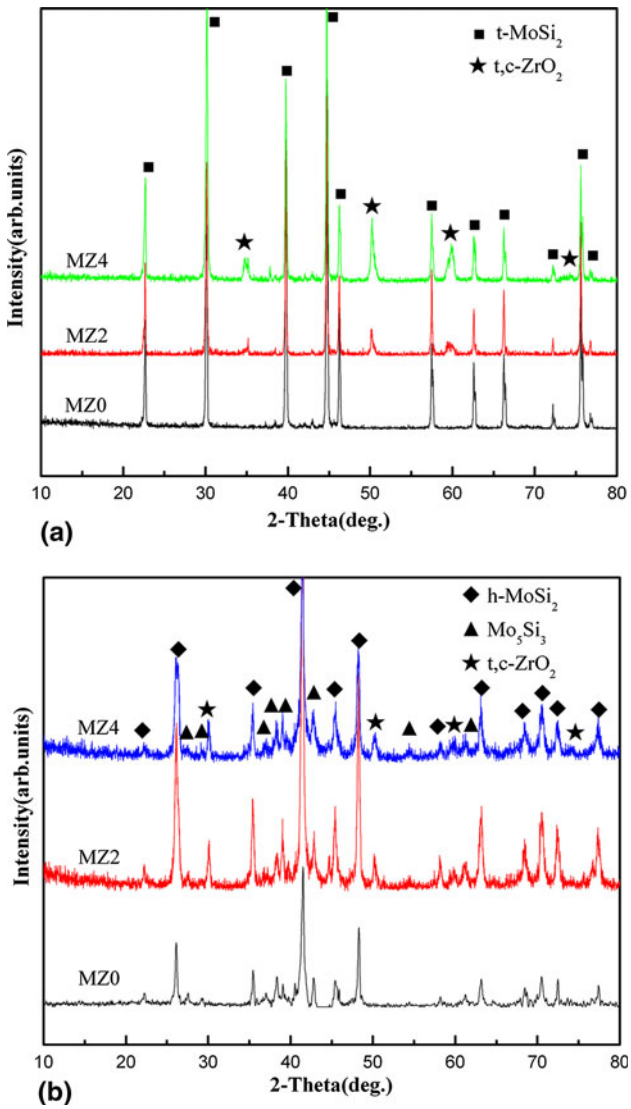

Fig. 1 XRD patterns of (a) $MoSi_2$-ZrO_2 powders and (b) corresponding plasma sprayed coatings

According to Eq 1, it was supposed that the existence of Mo_5Si_3 phase was caused by the chemical reaction between the melted $MoSi_2$ powders and residual oxygen in the vacuum chamber (pressure of the chamber: 100 mbar). Tetragonal and cubic ZrO_2 were still found in the XRD patterns of the MZ2 and MZ4 coatings, which revealed good chemical compatibility between $MoSi_2$ and ZrO_2.

$$5MoSi_{2(s)} + 7O_{2(g)} \rightarrow Mo_5Si_{3(s)} + 7SiO_{2(s)} \quad \text{(Eq 1)}$$

The surface morphologies of the as-sprayed $MoSi_2$ and $MoSi_2$-ZrO_2 composite coatings are shown in Fig. 2(a, c, and e). It can be seen that the surfaces of the MZ0 (Fig. 2a) and MZ2 (Fig. 2c) coatings were mostly composed of well-flattened splats. However, the MZ4 (Fig. 2e) coating presented a rougher surface which was constituted of insufficiently flattened protuberance and unmelted particles. The cross section SEM pictures of the as-sprayed coatings are given in Fig. 2(b, d, and f). Lamellar structure, which was a common character of plasma sprayed coatings, was observed in the MZ0 and MZ2 coatings. It was worth noticing that the MZ2 coating has a finer structure compared with that of the MZ0 coating. However, similar lamellar structure was not found for the MZ4 coating. It was supposed that the ZrO_2 powders were not easy to be fully molten due to its higher melting point compared with that of $MoSi_2$ (ZrO_2: 2700 °C, $MoSi_2$: 2030 °C), which led to the heterogeneity of the coating.

Some basic properties of the coatings, including porosity, microhardness, surface roughness, are summarized in Table 2. It can be seen that the MZ4 coating has the maximum surface roughness. The porosities of the MZ0, MZ2, and MZ4 coatings are 5%, 2%, and 4%, respectively. Microhardness of the as-sprayed MZ0, MZ2, and MZ4 coatings are 6.85 ± 0.80, 8.16 ± 0.94, and 6.63 ± 1.52 GPa, respectively. The results showed that the addition of 20 vol.% ZrO_2 reduced the porosity and

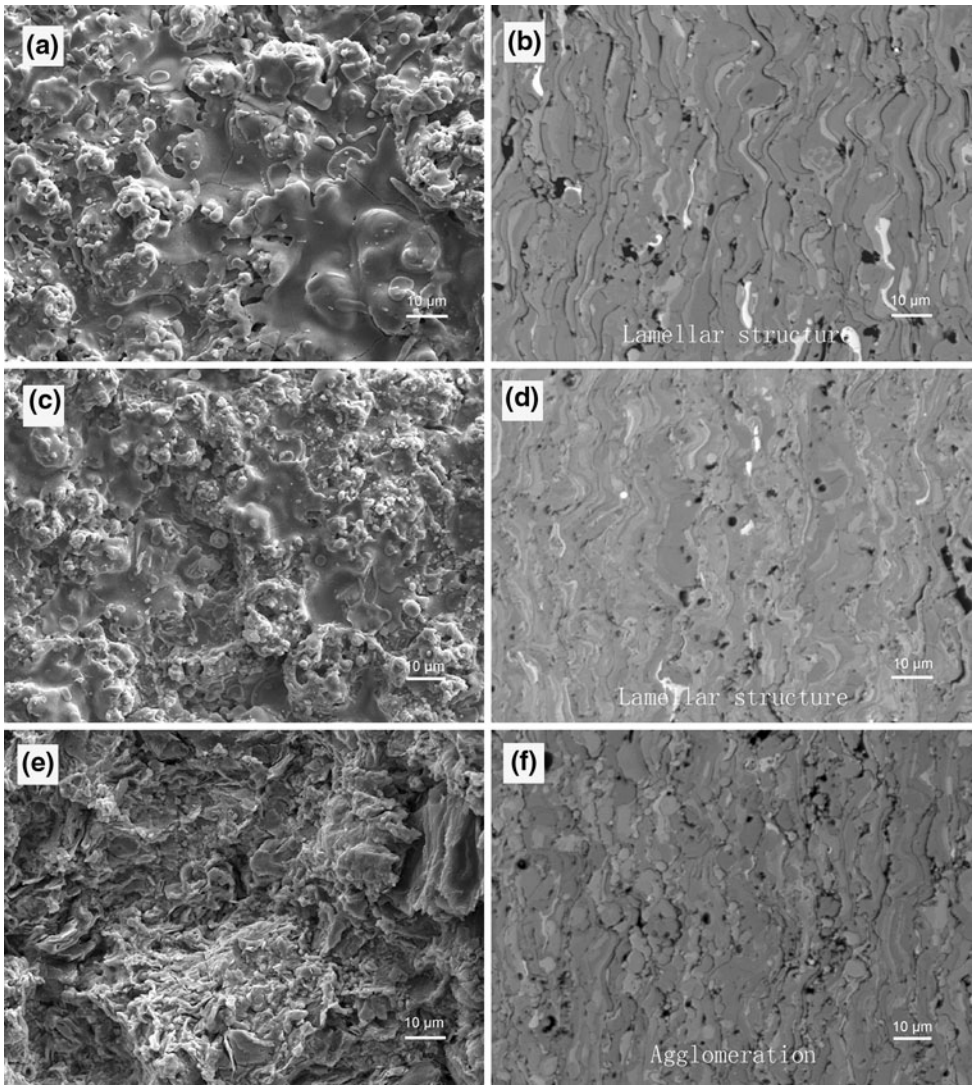

Fig. 2 Surface (a, c, e) and cross section (b, d, f) morphologies of the as-sprayed coatings: (a, b) MZ0, (c, d) MZ2, and (e, f) MZ4

Table 2 Properties of the as-sprayed coatings

Coatings	Porosity, %	Microhardness, GPa	Surface toughness, μm
MZ0	5	6.85 ± 0.80	3.71 ± 0.35
MZ2	2	8.16 ± 0.94	3.02 ± 0.34
MZ4	4	6.63 ± 1.52	5.48 ± 0.56

enhanced the microhardness of $MoSi_2$ coatings. Bhattacharya (Ref 9) prepared $MoSi_2$-ZrO_2 composites and examined their microstructure and mechanical property. They found that the addition of appropriate ZrO_2 progressively refined the grain size of $MoSi_2$ by retarding its grain growth during the crystallization, which improved the density and strength of $MoSi_2$. However, too much

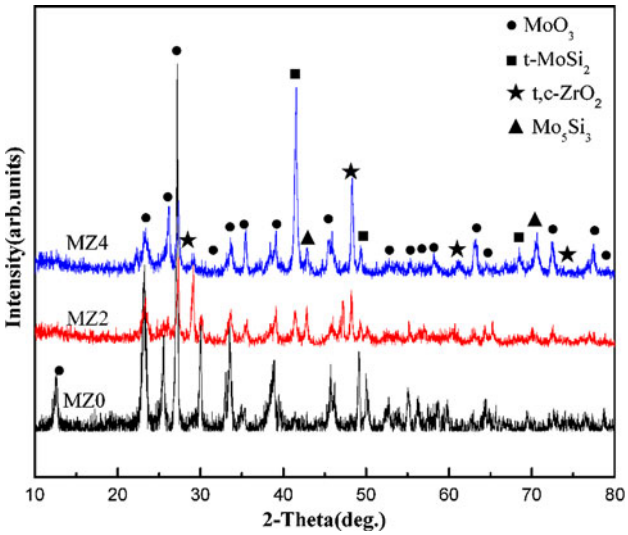

Fig. 3 XRD patterns of the MZ0, MZ2, and MZ4 coatings heated at 500 °C for 16 h

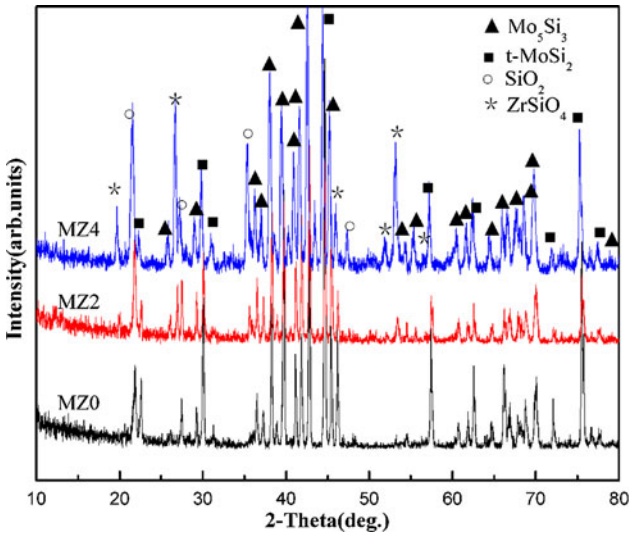

Fig. 5 XRD patterns of the MZ0, MZ2, and MZ4 coatings heated at 1200 °C for 50 h

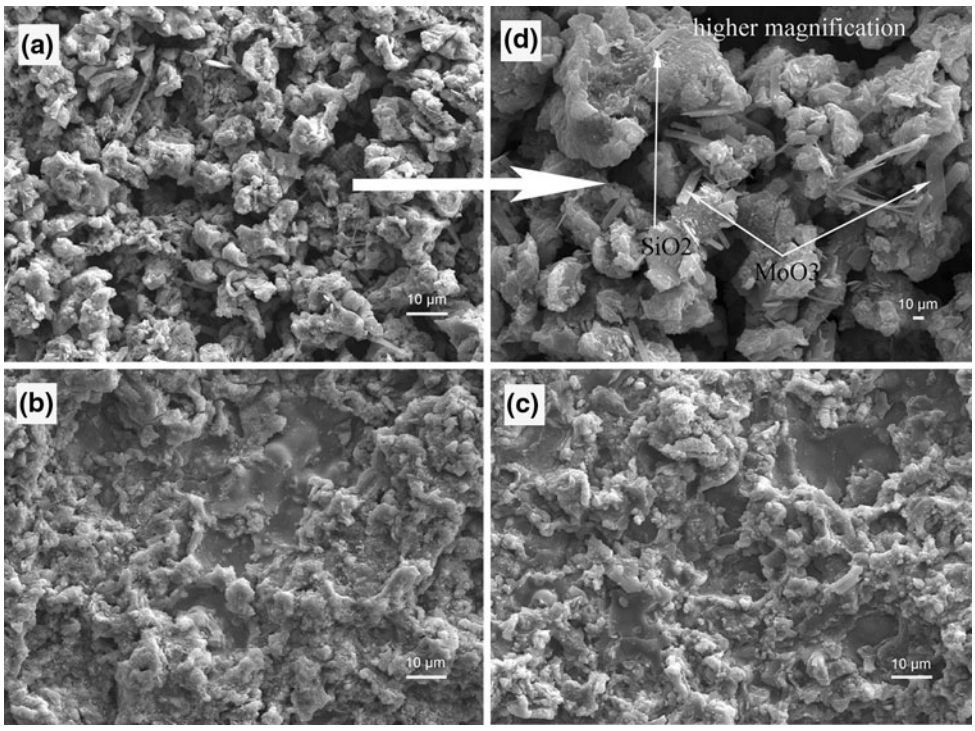

Fig. 4 Surface morphologies of the coatings heated at 500 °C for 16 h: (a) MZ0, (b) MZ2, (c) MZ4, and (d) higher magnification of (a)

ZrO_2 was found to be unevenly distributed in the $MoSi_2$ matrix and agglomeration phenomenon happened, which caused the heterogeneity of the mechanical properties.

3.2 Oxidation Behavior of the Coatings at 500 °C

The monolithic $MoSi_2$ is prone to oxidize through pores, cracks, and grain boundaries around 500 °C. It disintegrates into a green powder and their volumes increased extremely, which is known as the pest oxidation (Ref 11). At this temperature, $MoSi_2$ was oxidized by the reaction expressed as Eq 2. Solid MoO_3 impedes the formation of a dense protective SiO_2 scale and the molar volume increases by 250%.

$$2MoSi_{2(s)} + 7O_{2(g)} \rightarrow MoO_{3(s)} + 4SiO_{2(s)} \quad \text{(Eq 2)}$$

The XRD patterns of the coatings oxidized at 500 °C for 16 h are given in Fig. 3. MoO_3 was detected as the main phase in all the three coatings, a small amount of Mo_5Si_3 and residual tetragonal $MoSi_2$ were also found. However, the intensities of $MoSi_2$ peaks in the MZ2 and MZ4 coatings were much higher than that of the MZ0 coating. Figure 4 shows the surface morphologies of the MZ0, MZ2, and MZ4 coatings after being oxidized at 500 °C for 16 h. It was found that pest oxidation phenomenon took place in the MZ0 coating after 16 h oxidation as shown in Fig. 4(a). But it did not happen in the MZ2 and MZ4 coatings until 40 h. A higher magnification picture of Fig. 4(a) is given in Fig. 4(d) and many crystalline MoO_3-whiskers or platelets and amorphous SiO_2-clusters appeared in the MZ0 coating after 16 h heat treatment at 500 °C in air, which were the main products of pest oxidation (Ref 5). However, the surface pictures of MZ2 and MZ4 coatings (as shown in Fig. 4b, c) presented intact and dense microstructure, which indicated that the addition of ZrO_2 in $MoSi_2$ coating could restrain the pest oxidation of

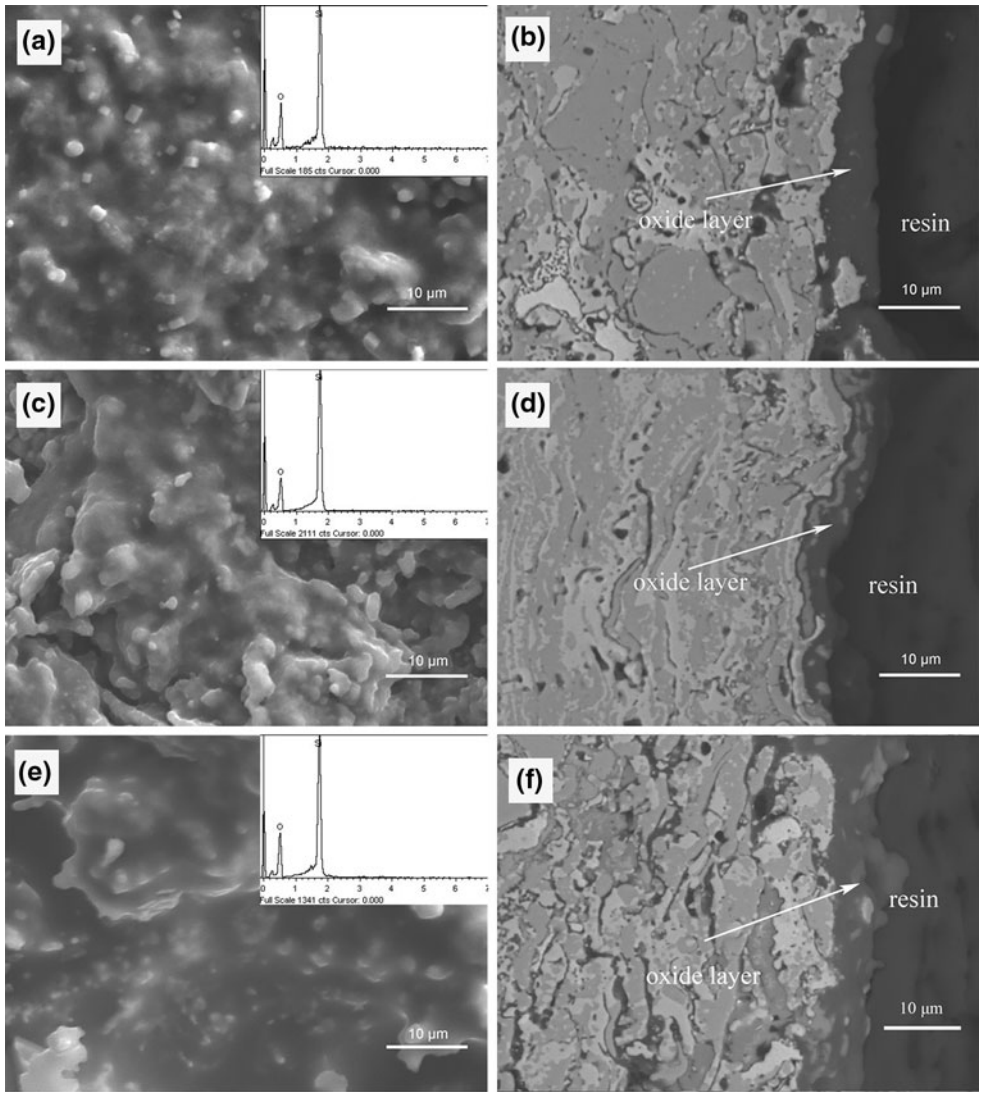

Fig. 6 Surface (a, c, e) and cross section (b, d, f) morphologies of the coatings heated at 1200 °C for 50 h: (a, b) MZ0, (c, d) MZ2, and (e, f) MZ4

$MoSi_2$ to some extent. Though the oxidation behavior of the coatings is related to the porosity at such low temperature, it has been proved that the addition of oxides could restrain the pest oxidation of $MoSi_2$ to some extent (Ref 12).

In previous studies (Ref 5), grain boundaries, defects such as pores and cracks have been considered important factors influencing the pest oxidation of $MoSi_2$. Wang et al. (Ref 13) found that the network microstructure of oxides was formed along the edges of grain boundaries of the $MoSi_2$ matrix. As a result, the paths of oxygen diffusion that caused pest oxidation were blocked and the low-temperature oxidation resistance was greatly improved. In the present study, the addition of ZrO_2 into $MoSi_2$ retarded the diffusion of oxygen and enhanced its low-temperature oxidation resistance. Besides, the porosities of the MZ2 and MZ4 coatings were lower than that of MZ0 coatings, which reduced the defects and contributed the inhibition of pest oxidation of the coatings.

3.3 Oxidation Behavior of the Coatings at 1200 °C

The coatings were oxidized at 1200 °C for 50 h to investigate the application of $MoSi_2$ composite coatings in the area of protecting high-temperature alloys. Figure 5 presents the XRD results of the oxidized coatings. Tetragonal $MoSi_2$, Mo_5Si_3, and SiO_2 were identified to be the main phases of all the three coatings, meanwhile, $ZrSiO_4$ was detected in the MZ2 and MZ4 coatings.

Figure 6(a, c, and e) illustrates the surface morphologies of the oxidized coatings, from which it can be observed that the surfaces of all the three kinds of coatings were mostly composed of glassy SiO_2. The polished cross section pictures of the oxidized coatings are given in Fig. 6(b, d, and f). The oxide layers with almost the same thickness were visible on the surfaces of the three kinds of coatings, indicating that the MZ2 and MZ4 coatings had comparable oxidation behavior to the $MoSi_2$ coating at 1200 °C.

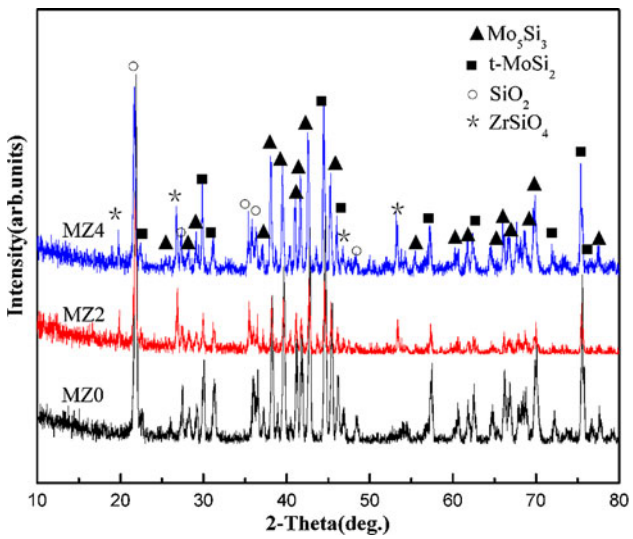

Fig. 7 XRD patterns of the MZ0, MZ2, and MZ4 coatings heated at 1500 °C for 7 h

3.4 Oxidation Behavior of the Coatings at 1500 °C

To investigate the potential application of $MoSi_2$ composite coatings at higher temperature, such as protective coatings for carbon/carbon composite, the oxidation behavior of the coatings around 1500 °C was also processed (Ref 4). The MZ0, MZ2, and MZ4 coatings were oxidized at 1500 °C for 7 h. The XRD patterns of the oxidized coatings are illustrated in Fig. 7. It was found that the diffraction intensity of SiO_2 phase increased as compared with those in the 1200 °C tests (Fig. 5). The $ZrSiO_4$ phase was also detected in the $MoSi_2$-ZrO_2 composite coatings. The surface morphologies of the oxidized coatings are shown in Fig. 8(a, c, and e). Glassy SiO_2 were also observed for all the three kinds of coatings. The cross section morphologies of the oxidized coatings are given in Fig. 8(b, d, and f), which revealed that both of the MZ0 and MZ2 coatings maintained dense surface oxidation film with thicknesses less than 10 μm which indicating the excellent oxidation resistance of the coatings. However, a thick-oxide layer of more than 30 μm having a loose structure with many pores formed on the surface of the MZ4 coating. Most publications agreed that the formation temperature of $ZrSiO_4$ varied between 1300 and 1700 °C, resulting in different published phase diagrams (Ref 14). Suzuki et al. (Ref 15) demonstrated that the formation of $ZrSiO_4$ started from ZrO_2 and SiO_2 was accompanied with a large volume change causing the formation of voids (up to 10 vol.%) in the coatings. In the MZ4 coating, most of ZrO_2 reacted with thermally grown SiO_2 of $MoSi_2$ to form $ZrSiO_4$ by the heat treatment. This process consumed too much protective glassy SiO_2 and also accompanied with a large volume change (Ref 16). Thus the voids were formed in the MZ4 coating heated at 1500 °C; however, they were not found at 1200 °C.

4. Conclusions

$MoSi_2$-ZrO_2 composite coatings were fabricated by VPS method. It was found that the addition of 20 vol.% ZrO_2 in $MoSi_2$ reduced the porosity and enhanced the microhardness of $MoSi_2$ coatings. The addition of ZrO_2 could restrain pestoxidation of plasma sprayed $MoSi_2$ coatings to some extent at low temperature (around 500 °C). $MoSi_2$-20 vol.% ZrO_2 composite coatings maintained excellent oxidation resistance both at 1200 and 1500 °C. However, ZrO_2 content (40 vol.%) in the $MoSi_2$ coating could impair oxidation resistance of the coating at 1500 °C owing to the volume change caused by the decomposition of $ZrSiO_4$, though the comparable oxidation property at 1200 °C was still obtained.

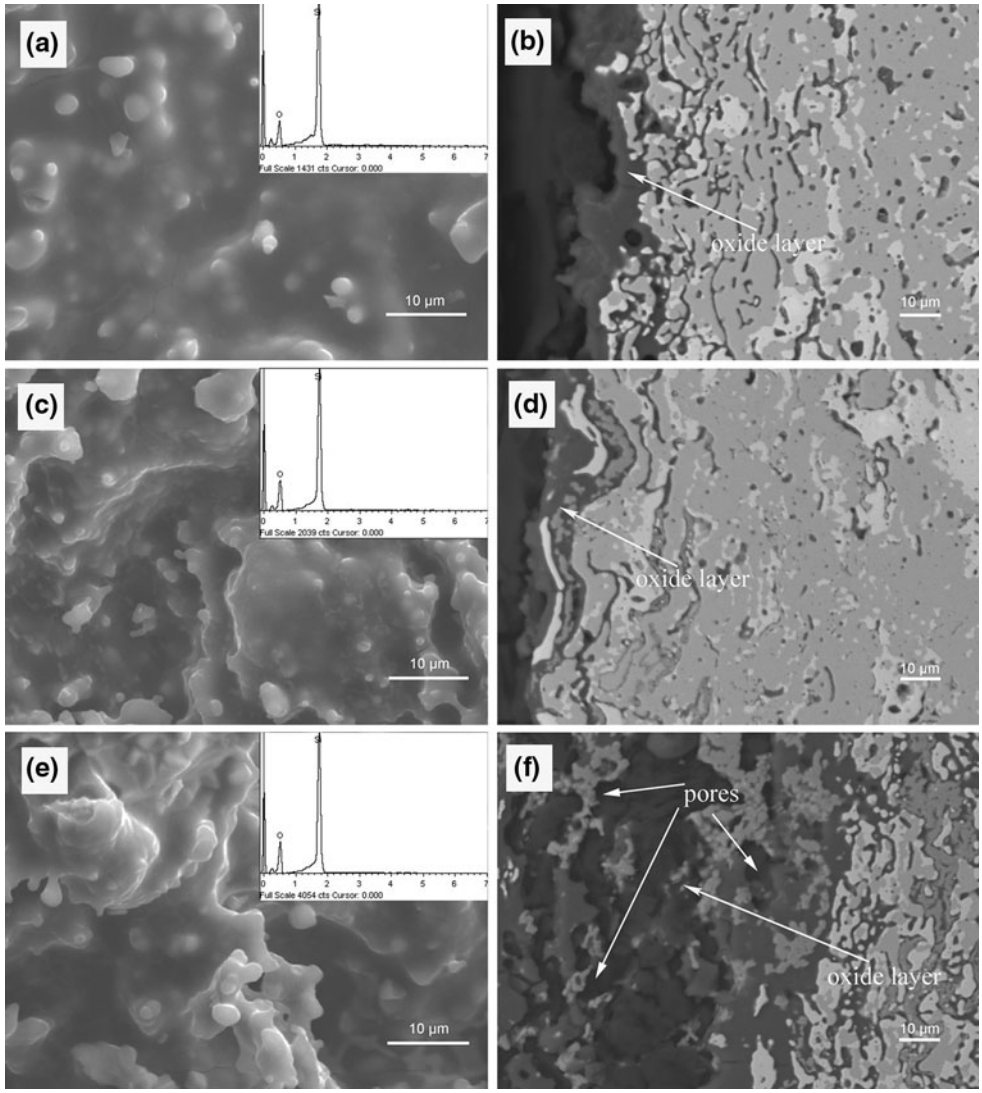

Fig. 8 Surface (a, c, e) and cross section (b, d, f) morphologies of the coatings heated at 1500 °C for 7 h: (a, b) MZ0, (c, d) MZ2, and (e, f) MZ4

References

1. R. Tiwari, H. Herman, and S. Sampath, Vacuum Plasma Spraying of $MoSi_2$ and Its Composite, *Mater. Sci. Eng. A*, 1992, **155**, p 95-100
2. M. Zakeri, R. Yazdani-Rad, M.H. Enayati, and M.R. Rahimipoor, Synthesis of $MoSi_2$-Al_2O_3 Nanocomposite by Mechanical Alloying, *Mater. Sci. Eng. A*, 2006, **430**, p 185-188
3. A.K. Vasudévan and J.J. Petrovic, A Comparative Overview of Molybdenum Disilicide Composites, *Mater. Sci. Eng. A*, 1992, **155**, p 1-17
4. E.K. Nyutu, M.A. Kmetz, and S.L. Suib, Formation of $MoSi_2$-SiO_2 Coatings on Molybdenum Substrates by CVD/MOCVD, *Surf. Coat. Technol.*, 2006, **200**, p 3980-3986
5. T.A. Kircher and E.L. Courtright, Engineering Limitations of $MoSi_2$ Coatings, *Mater. Sci. Eng. A*, 1992, **155**, p 67-74
6. R.G. Castro, H. Kung, and P.W. Stanek, Reactive Plasma Spraying of $MoSi_2$ Using an Ar-10% CH_4 Powder Carrier Gas, *Mater. Sci. Eng. A*, 1994, **185**, p 65-70
7. T.C. Chou and T.G. Nieh, Mechanism of $MoSi_2$ Pest During Low Temperature Oxidation, *J. Mater. Res.*, 1993, **8**, p 214-226
8. S. Lohfeld and M. Schütze, Oxidation Behaviour of Particle Reinforced $MoSi_2$ Composites at Temperatures Up to 1700°C: Part I: Literature Review, *Mater. Corros.*, 2005, **56**, p 93-97
9. A.K. Bhattacharya, Microstructure and Mechanical Properties of 2.5 Yttria Partially Stabilized Zirconia-Reinforced Molybdenum Disilicide Composites, *J. Mater. Sci. Lett.*, 1993, **12**, p 372-374
10. J.J. Petrovic and R.E. Honnell, Partially Stabilized ZrO_2 Particle-$MoSi_2$ Matrix Composites, *J. Mater. Sci.*, 1990, **25**, p 4453-4456
11. G. Reisel, B. Wielage, S. Steinhäuser, I. Morgenthal, and R. Scholl, High Temperature Oxidation Behavior of HVOF-Sprayed Unreinforced And Reinforced Molybdenum Disilicide Powders, *Surf. Coat. Technol.*, 2001, **146**, p 19-26
12. P.J. Meschter, Oxidation of $MoSi_2/TiB_2$ and $MoSi_2/Al_2O_3$ mixtures, *Scripta Mater.*, 1991, **25**, p 1065-1069
13. G. Wang, W. Jiang, G. Bai, and L. Wu, Effect of Addition of Oxides on Low-Temperature Oxidation of Molybdenum Disilicide, *J. Am. Ceram. Soc.*, 2003, **86**(4), p 731-734
14. A. Kaiser, M. Lobert, and R. Telle, Thermal Stability of Zircon ($ZrSiO_4$), *J. Eur. Ceram. Soc.*, 2008, **28**, p 2199-2211
15. M. Suzuki, S. Sodeoka, and T. Inoue, Zircon-Based Ceramics Composite Coating for Environmental Barrier Coating, *J. Thermal Spray Tech.*, 2008, **17**(3), p 404-409
16. Y. Tange and E. Takahashi, Stability of the High-Pressure Polymorph of Zircon ($ZrSiO_4$) in the Deep Mantle, *Phys. Earth Planet. Inter.*, 2004, **143**, p 223-229